

# Experimental study and modelling of gelatin production from bone powder: elaboration of an overall kinetic scheme for the acid process

M.-O. Nicolas-Simonnot <sup>a,\*</sup>, V. Tréguer <sup>a</sup>, J.-P. Leclerc <sup>a</sup>, M. Sardin <sup>a</sup>, J.-P. Brajoux <sup>b</sup>, J. Moy <sup>b</sup>,  
G. Takerkart <sup>b</sup>

<sup>a</sup> *Laboratoire des Sciences du Génie Chimique, ENSIC-CNRS, 1 rue Grandville, BP 451, 54001 Nancy Cedex, France*

<sup>b</sup> *S.B.I., Moulins Premiers, BP 23, 84800 Isle-s-Sorgue, France*

Received 12 December 1996; accepted 30 January 1997

## Abstract

This paper deals with the production of gelatin by acid extraction from animal bones. Experimental data show that during the extraction the “extraction yield” and the mean molecular weight reach a maximum and then decrease, which is attributable to chain degradation. The purpose of this paper is to establish a kinetic scheme that can be included in a global process model able to predict both the yield and the quality (molecular weight) of the gelatin produced.

We propose an experimental study of the extraction from hard bones for different particle sizes at 75 °C and pH 2.25 and an interpretation of the results by means of the shrinking core model: it is shown that the kinetic limitations are chemical ones and a kinetic constant is computed.

A detailed study of the influence of temperature and pH on extraction and degradation (60–85 °C, pH 1.75–2.50) is then presented. A model is proposed: gelatin products are represented by four classes, and the kinetic laws for extraction and degradation are determined; parameters are computed from experimental data.

The overall kinetic scheme can predict the main trends observed for acid production of gelatin and can be included in a process model.  
© 1997 Elsevier Science S.A.

*Keywords:* Acid process; Gelatin production; Kinetic modelling; Shrinking core model

## 1. Introduction

Gelatin manufacture was developed in the early 1920s, but the process is still of great interest given the important industrial applications of gelatin in many fields, such as photography, food, pharmacy, etc. The product must generally fulfil stringent quality requirements [1].

Gelatin is made up of a series of polypeptide chains stemming from collagen denaturation. The basic element is the so-called “ $\alpha$  chain” with a molecular weight of 95 000; this chain may be involved in degradation or association and may form products of lower or higher weight. A high molecular weight is among the criteria of gelatin quality.

At present, two main processes [1–8] are used to extract gelatin from animal raw materials (e.g. skins and bones): an alkaline process, giving high quality products for photographic applications, and an acid process, which is faster but leads to a lower quality product for food use. This lower

quality is related to a lower mean molecular weight, caused by chain degradation reactions interfering with the gelatin extraction.

Papers about gelatin and its applications are available (e.g. [9,10]) but few of them deal with the processes. An experimental study of the extraction process reported in [3] is concerned mainly with the effects of temperature and pH on the yield and the molecular weight distribution. It is shown that temperature plays the most important role: a temperature increase leads to a higher yield, but molecular weights increase to a maximum and then drop, because of chain degradation. A model for the kinetics of bone demineralization, supported by experiments, has been presented by Markarewicz et al. [11]. Briefly speaking, everything concerning the control and modelling of gelatin production is currently of interest.

The overall objective of our work is the development of a kinetic model for the process of acid extraction of gelatin from crushed bones: this model must fit the known data. The aim is not to develop highly detailed aspects regarding the physico-chemistry of gelatin, but to highlight the main trends.

\* Corresponding author. Tel.: +33 3 83 17 50 00; fax: +33 3 83 32 29 75.

Our work comprises two steps:

- A first experimental study of acid extraction of gelatin performed with a given bone quality at fixed temperature and pH, for different particle sizes. Experimental results are handled in the frame of a well known chemical engineering model: the shrinking-core model. This enables us to determine the limiting step and to compute an overall kinetic constant.
- The second part is devoted to a more detailed approach, aimed at the derivation of an overall reaction scheme describing both extraction and degradation. It is assumed that the reaction products are divided into four classes according to their molecular weight. Kinetic constants of extraction and degradation are then estimated, taking account of the effects of pH and temperature (65–80 °C, pH 1.75–2.25). The overall reaction scheme can be included in a global model describing the continuous acid process, which is able to predict the evolution of the different product classes and thus the product quality.

## 2. Materials and methods

In the first part, experiments on gelatin extraction from hard bones, performed at 75 °C and pH 2.25 with different particle sizes, are presented. The second part focuses on the influence of temperature and pH on the production rate and on the mean molecular weight of the gelatin.

### 2.1. Gelatin extraction from hard bones: influence of the particle size

Hard bones (see Table 1) were chosen because the particles obtained after crushing and sieving are uniform in composition and structure, independent of their granulometry (porous bone fragments would have a highly non-uniform structure). Experiments were performed with three size ranges (Table 2). Particle diameters were kept below  $\approx 2$  mm because earlier results had shown that low extraction yields were obtained with larger pellets, and furthermore these fine particles are generally not used but are considered as waste.

The first step consists in demineralization of the bones: in a glass batch reactor, 600 g of bone powder are mixed with hydrochloric acid (4.4 l, 50 g l<sup>-1</sup>) at room temperature for 1 h to dissolve inorganic materials (mainly calcium phosphate): this produces wet ossein (1500 g). After filtration, this ossein is washed three times with tap water (5 l) for half an hour. Samples are taken to determine the water content (85%) and the hydroxyproline content (7%) of dry ossein. Hydroxyproline is a major component (see amino acid composition, Table 3) and measurement of the hydroxyproline fraction gives the total mass of extractable gelatin contained in ossein.

The second step comprises the actual extraction of gelatin. Wet ossein is mixed with demineralized water for 1 h at

Table 1  
Composition of hard bones

Components	Weight %
Ca <sub>3</sub> (PO <sub>4</sub> ) <sub>2</sub>	52
Proteins	29
Mineral salts	12
Fats	1
Water	6

Table 2  
Size ranges of bone particles used in the experiments

	Radius size range/mm	Mean radius/mm
No. 1	0.125-0.250	0.188
No. 2	0.500-0.700	0.600
No. 3	0.700-0.800	0.750

Table 3  
Amino acid composition of gelatin

Components	Weight %
Glycine	27
Proline	16
Hydroxyproline	14
Alanine	9
Glutamic acid	12
Arginine	8
Aspartic acid	6
Others	8

controlled temperature (75 °C) and pH (2.25) in a 4 l glass batch reactor (mixer: diameter 60 mm). The pH is controlled by addition of phosphoric acid. The stirring speed is increased during the reaction because of the increase in viscosity: the ossein must be in suspension. Samples (5 ml) are taken during extraction and centrifuged: the solid fraction is reinjected into the reactor and the supernatant is analysed by refractometry (immediately after sampling) to determine the gelatin content and the extraction yield. The refractometer (manual refractometer from Atago) has a range of 0–20% Brix, and the correlation used to obtain the gelatin concentration (determined at S.B.I.) is

Concentration of gelatin (gl<sup>-1</sup>) = 6.81 × (% from refractometry).

Fig. 1 shows the experimental variations of the extraction yield  $X_B$  with time for the three bone samples.  $X_B$  = (mass of extracted gelatin) / (mass of extractable gelatin).

### 2.2. Investigation of the influence of temperature and pH

For this part of the work, the raw material was chosen to be very close to the actual materials used for gelatin production: it comprised a mixture of different cattle bone qualities (not only hard bones), especially the particle fraction with diameter < 2 mm, and the mean radius was 0.37 mm. A set of 16 experiments (Table 4) was performed.

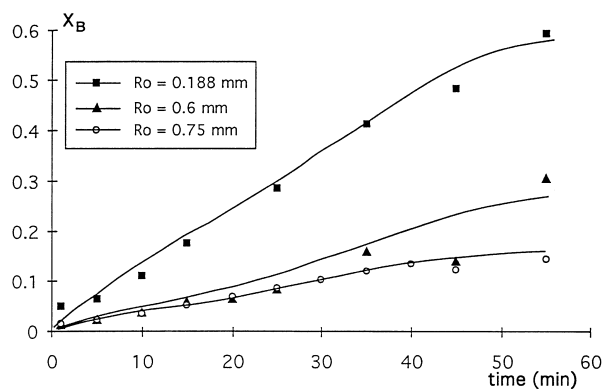


Fig. 1. Evolution of the extraction yield with time for three nominal size ranges; pH = 2.25, temperature 75 °C.

Table 4  
Experimental conditions of temperature and pH

pH	1.75	2.00	2.25	2.50
T/ °C				
65	E1	E2	E3	E4
70	E5	E6	E7	E8
75	E9	E10	E11	E12
80	E13	E14	E15	E16

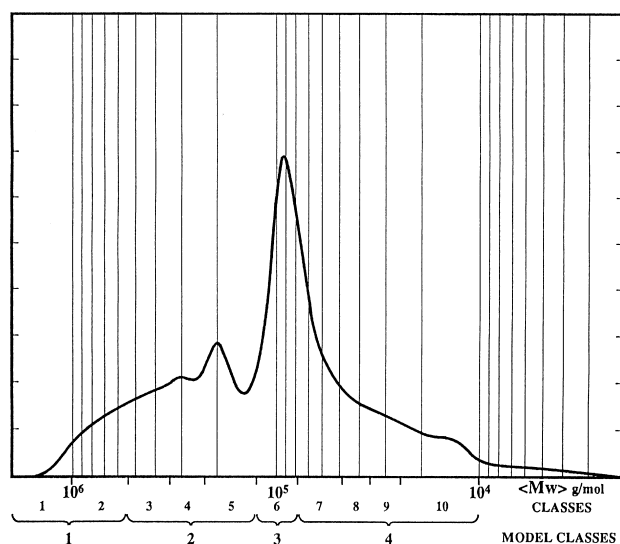


Fig. 2. An example of a chromatogram of gelatin: definition of the four classes.

Extraction is carried out as explained earlier, and degradation is investigated at pH 2.25 for experiments E7, E11 and E15: samples are taken during extraction, ossein is removed, and the remaining aqueous solutions are maintained at the same temperature and pH as for extraction. The molecular weight distribution is then measured at different times by gel permeation chromatography. A typical chromatogram is shown in Fig. 2. Molecular weights have a distribution from  $<10\,000$  to  $>500\,000$  g mol<sup>-1</sup>. The exploitation software allocates the distribution to 10 categories of product with decreasing molecular weights. During degradation the

expected evolution is revealed: the distribution moves towards lower weights.

### 3. Determination of the limiting step for the extraction process: chemistry or diffusion?

#### 3.1. Model presentation

For the first experimental part, given that particle diameter is constant during extraction, the reaction may proceed in shrinking-core fashion. The general features of this model are described in many literature sources, e.g. [12–14]. It is applied when solid particles are composed of a core of reacting material surrounded by a reacted shell; the core shrinks as the reaction front proceeds within the particle. Markarewicz et al. [11] modelled the kinetics of bone demineralization with this approach.

Let us recall its basic principles. A typical reaction is



where A is the hydronium ion, B is gelatin attached to ossein, and the product is gelatin in solution.

Particles are assumed to be spherical, characterized by their radius  $R_0$  and the core radius  $R$ , which decreases from  $R_0$  to zero. The reaction occurs in five steps:

1. diffusion of A from the bulk solution to the particle surface through the external film around the particle;
2. diffusion of A through the reacted shell to the reactive front;
3. reaction at the core surface;
4. diffusion of products through the reacted shell to the external surface;
5. diffusion of products through the external film to the bulk solution.

Here, it is very probable that steps 4 and 5 are not rate-controlling because the penetration of acid makes the bone particles become very porous, so that reaction products can easily be transferred to the solution. From the experimental data, it will be determined whether one of the steps 1, 2 and 3 is rate-controlling.

#### 3.1.1. Case 1: chemical reaction is rate-controlling

It was previously observed that the extraction yield was independent of the initial concentration of gelatin in bones. In fact, the reaction is a dissolution and its rate does not depend on the ossein concentration. The rate decreases with time because of the reduction in the reaction area. It can be assumed that extraction is actually dissolution and thus a zero-order reaction with respect to gelatin. We may recall that pH and temperature are constant. The gelatin mass balance is then

$$\frac{dm_B}{dt} = -k4\pi R^2 \quad (1)$$

where  $k$  is the extraction rate constant ( $\text{kg s}^{-1} \text{m}^{-2}$ ),  $m_B$  is the mass of gelatin in the particle at time  $t$  (kg), and  $R$  is the core radius (m).

The relationship between  $R$ ,  $m_B$  and  $X_B$  (current conversion) can be referred to mass, to mole or to volume, for example

$$X_B = 1 - \left(\frac{R}{R_0}\right)^3 = 1 - \frac{m_B}{m_{B_0}}$$

Then Eq. (1) yields

$$\frac{dX_B}{dt} = \frac{3k}{\rho_B R_0} (1 - X_B)^{\frac{2}{3}} \quad (2)$$

where  $\rho_B$  is the apparent ossein density ( $\text{kg m}^{-3}$ ) and assumed constant.

The integration of Eq. (2) from the initial to the current time yields

$$\frac{t}{\lambda_1 R_0} = 1 - (1 - X_B)^{\frac{1}{3}} \quad (3)$$

with

$$\lambda_1 = \frac{\rho_B}{k}$$

### 3.1.2. Case 2: external diffusion is rate-controlling

In the pseudo steady-state assumption, molar fluxes are imposed to be equal at any location inside the particle. The molar flux of A transferred from the bulk solution is

$$F_A = k_d 4\pi R_0^2 (C_A - C_{AS}) \approx k_d 4\pi R_0^2 C_A \quad (4)$$

where  $k_d$  is the external transfer conductance ( $\text{m s}^{-1}$ ),  $C_A$  is the concentration of A in the bulk solution ( $\text{mol m}^{-3}$ ),  $C_A$  is assumed constant, and  $C_{AS}$  is the concentration of A at the external particle surface ( $\text{mol m}^{-3}$ );  $C_{AS} \approx 0$  if the resistance is located in the external film.

From Eq. (4), the molar flux equality leads to

$$\frac{dX_B}{dt} = \frac{3M_B k_d}{\rho_B R_0} C_A \quad (5)$$

where  $M_B$  is the mean molecular weight of gelatin ( $\text{kg mol}^{-1}$ ).

$k_d$  may be expressed by classical chemical engineering correlations [15]

$$\text{Sh} = \frac{k_d(2R_0)}{D_A} = 2 + 0.6\text{Re}^{\frac{1}{2}}\text{Sc}^{\frac{1}{3}} \quad (6)$$

where  $D_A$  is the molecular diffusivity ( $\text{m}^2 \text{s}^{-1}$ ),  $\text{Re}$  is the Reynolds number, and  $\text{Sc}$  is the Schmidt number.

In turbulent flow, the second term of Eq. (6) is predominant and  $k_d$  is proportional to  $R_0^{-1/2}$

$$k_d = \gamma R_0^{-\frac{1}{2}} \quad (7)$$

Thus the integration of Eq. (6) leads to

$$\frac{t}{\lambda_2 R_0^{3/2}} = X_B \quad (8)$$

with

$$\lambda_2 = \frac{\rho_B}{3M_B \gamma C_A}$$

### 3.1.3. Case 3: internal diffusion is rate-controlling

The supply of A is limited by the diffusion through the reacted shell. Let  $D_e$  be the effective diffusivity of A in the particle; then the molar flux of A at radius  $R$  is

$$F_A = 4\pi D_e \frac{R_0 R}{R_0 - R} C_A \quad (9)$$

External transfer and reaction are considered to be fast processes, so that the A concentration equals the bulk concentration at the external surface  $R_0$  and tends to zero at the reaction front

$$\frac{dX_B}{dt} = \frac{3M_B C_A D_e}{\rho_B R_0^2} \frac{(1 - X_B)^{\frac{1}{3}}}{1 - (1 - X_B)^{\frac{2}{3}}} \quad (10)$$

Integration of Eq. (10) yields

$$\frac{t}{\lambda_3 R_0^2} = 1 + 2(1 - X_B) - 3(1 - X_B)^{\frac{2}{3}} \quad (11)$$

with

$$\lambda_3 = \frac{\rho_B}{6M_B C_A D_e}$$

Eqs. (3), (8) and (11) are written in order that their denominator represents the total consumption time required ( $X_B = 1$ ) for each case.

## 3.2. Results and discussion

Each relationship, Eqs. (3), (8) and (11), involves one parameter ( $\lambda_i$ ) $_{1 \leq i \leq 3}$ , since  $k$ ,  $\gamma$  and  $D_e$  are unknown. Each  $\lambda_i$  was optimized on the three curves simultaneously by the Box method [16]. As an illustration, the experimental and calculated variations of  $1 - (1 - X_B)^{1/3}$ ,  $X_B$  and  $1 + 2(1 - X_B) - 3(1 - X_B)^{2/3}$  respectively are plotted against time in Figs. 3–5. The calculated curves were obtained with the following optimized parameters:

$$\begin{aligned} \lambda_1 &= 7.02 \times 10^7 \text{ s m}^{-1} \\ \lambda_2 &= 1.93 \times 10^9 \text{ s m}^{-3/2} \\ \lambda_3 &= 6.60 \times 10^{11} \text{ s m}^{-2} \end{aligned}$$

From these values, the case in which chemical kinetics is the controlling process appears to fit best to the experimental results. The optimized  $\lambda_1$  value leads to the rate constant

$$k = 6.36 \times 10^{-6} \text{ kg s}^{-1} \text{ m}^{-2}$$

with  $\rho_B = 446.5 \text{ kg m}^{-3}$ .

Fairly good agreement is achieved between the experimental data and model predictions in this case. This seems to

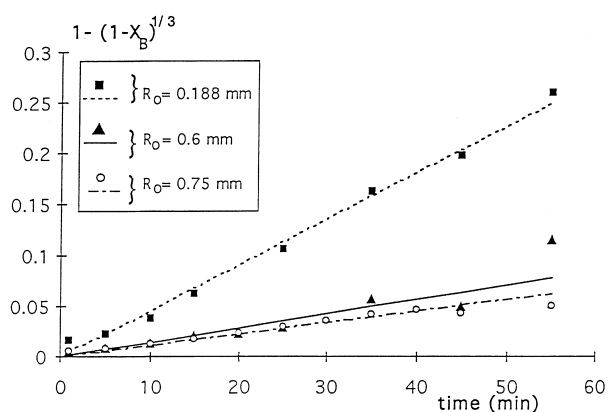


Fig. 3. Experimental and calculated evolution of  $1 - (1 - X_B)^{1/3}$  with time when chemical reaction is considered to be rate-controlling ( $\lambda_1 = 7.20 \times 10^7 \text{ s m}^{-1}$ ).

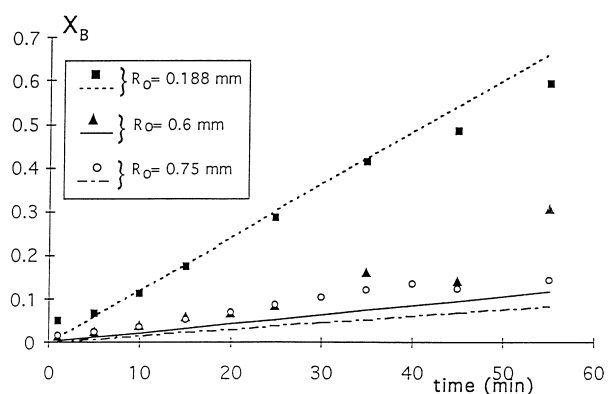


Fig. 4. Experimental and calculated evolution of  $X_B$  with time when external diffusion is considered to be rate-controlling ( $\lambda_2 = 1.93 \times 10^9 \text{ s m}^{-3/2}$ ).

confirm the validity of the assumption of a zero-order reaction.

Conversely, in the other two situations, poor agreement is obtained

For external diffusion control, given the form of the  $X_B$  curves (Fig. 4), Eq. (8), which is a linear function of time, cannot represent the experimental variations of  $X_B$ . This can be explained by the experimental conditions: experiments were performed with efficient stirring, so that external mass transfer effects were minimized.

In respect of internal diffusion, it is worth noting that bone particles after demineralization are rather porous, so that the diffusion of acid through the reacted solid is not limiting.

## 4. Development of a kinetic scheme describing both extraction and degradation

### 4.1. Assumptions

The objective is the development of a kinetic scheme simple enough to be integrated in an overall description of the process but complete enough to give the main trends. This is possible because diffusional limitations are negligible. We could start from the 10 classes of products shown by the

chromatograms, but it would be difficult to account for all these classes (too many reactions of extraction and degradation). Consequently, it is assumed that the products can be divided into four main classes. This classification is based on the existence of a ‘‘basic pattern’’: the  $\alpha$  chain, with a molecular weight of  $95\,000 \text{ g mol}^{-1}$ . The four categories are then:

class 1 ( $M_{w1} = 700\,000 \text{ g mol}^{-1}$ ): macromolecules with a molecular weight greater than  $500\,000 \text{ g mol}^{-1}$ , resulting from an association of at least five  $\alpha$  chains;  
class 2 ( $M_{w2} = 240\,000 \text{ g mol}^{-1}$ ): chains with a weight between  $120\,000$  and  $500\,000 \text{ g mol}^{-1}$  (up to five  $\alpha$  chains);  
class 3 ( $M_{w3} = 100\,000 \text{ g mol}^{-1}$ ):  $\alpha$  chains between  $80\,000$  and  $120\,000 \text{ g mol}^{-1}$ ;  
class 4 ( $M_{w4} = 35\,000 \text{ g mol}^{-1}$ ): shorter chains, from  $10\,000$  to  $80\,000 \text{ g mol}^{-1}$ .

The application-related properties of gelatin depend on the ratios of the different categories. The gelling rate increases with the ratio of the first two classes, the third category ( $\alpha$  chains) favours gel strength, as smaller chains contribute to make the gelling rate and gel strength decrease. Consequently, our model will have to predict not only the conversion and the mean molecular weight but also the ratio of the different weight categories of macromolecules in order to predict the properties in application.

The overall kinetic scheme is based on four assumptions:

1. all the classes of macromolecules are produced from ossein by first-order reactions (extraction);
2. the macromolecules in classes 1–3 are likely to degrade to give smaller chains of lower classes. Degradation reactions are considered to be first-order;
3. extraction and degradation depend a priori on temperature and pH. These parameters are kept constant during each experiment;
4. the total volume is constant.

From assumption 2, three degradation reactions may occur

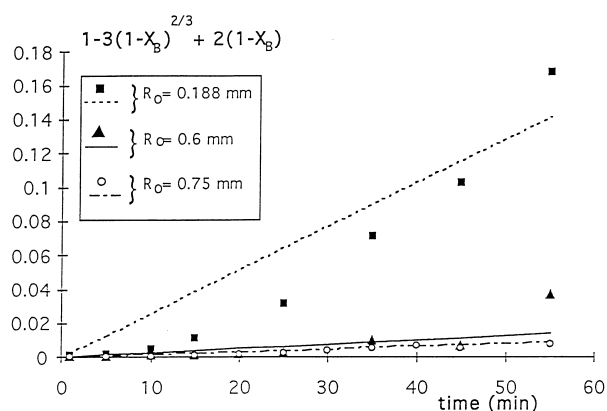


Fig. 5. Experimental and calculated evolution of  $1 + 2(1 - X_B)^{2/3} - 3(1 - X_B)^{1/3}$  with time when internal diffusion is considered to be rate-controlling ( $\lambda_3 = 6.60 \times 10^{11} \text{ s m}^{-2}$ ).

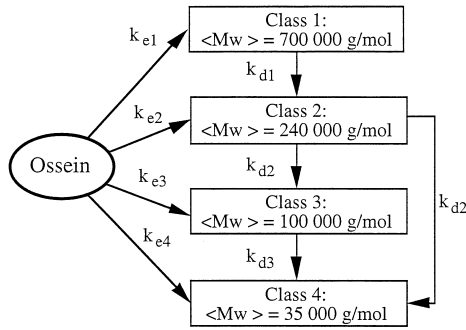


Fig. 6. Overall kinetic scheme.

The stoichiometric coefficients  $\nu_{ij}$  must take account of mass balances and should be as simple as possible to limit the number of optimized parameters. The following reactions are then chosen



The overall kinetic scheme is given in Fig. 6. Gelatin production is represented by seven reactions for which the kinetic constant must be determined:

four extraction reactions: macromolecule ‘‘release’’ from ossein pellets,  
three degradation reactions: transformation of high weight macromolecules into smaller chains.

Given that extraction cannot occur without degradation, degradation is investigated first and the constants will be used for the determination of the extraction constants.

#### 4.2. Determination of the kinetic constants of degradation reactions

For the sake of simplicity, these reactions are considered to be first-order. The mass balances in a batch reactor then yield

$$\frac{d\rho_1}{dt} = -k_{d1}\rho_1 \quad (18)$$

$$\frac{d\rho_2}{dt} = 3\frac{\bar{M}_{w2}}{\bar{M}_{w1}}k_{d1}\rho_1 - k_{d2}\rho_2 \quad (19)$$

$$\frac{d\rho_3}{dt} = 2\frac{\bar{M}_{w3}}{\bar{M}_{w2}}k_{d2}\rho_2 - k_{d3}\rho_3 \quad (20)$$

$$\frac{d\rho_4}{dt} = \frac{\bar{M}_{w4}}{\bar{M}_{w2}}k_{d2}\rho_2 + 3\frac{\bar{M}_{w4}}{\bar{M}_{w3}}k_{d3}\rho_3 \quad (21)$$

These mass balances can be written in terms of conversion independently of concentrations, which agrees with the findings of Northrop and Aren quoted by Veis [17]: they observed that the initial degradation rate did not depend on gelatin concentration.

Previous results had shown that the degradation rate did not depend on pH (in the investigated pH range). An example

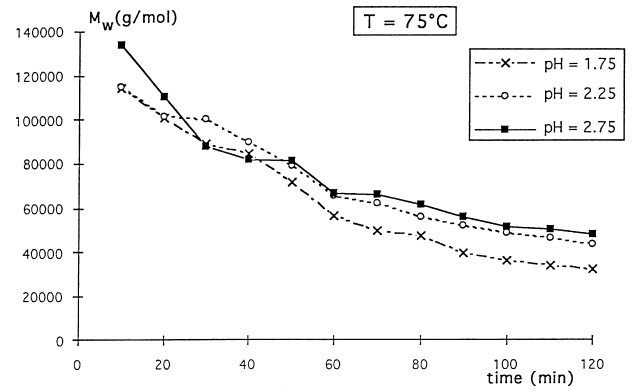


Fig. 7. Average molecular weight of gelatin versus time for different pH values during a degradation experiment performed at 75 °C.

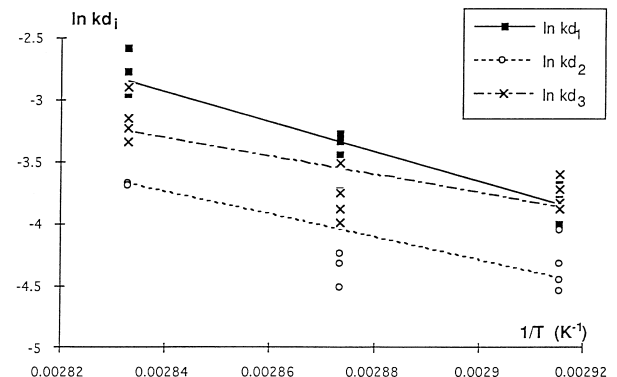


Fig. 8. Determination of the activation energy of the degradation reactions: plot of the logarithms of the rate constants of degradation reactions versus the inverse of temperature.

is presented in Fig. 7: for degradation experiments performed at 75 °C, the evolution of the mean molecular weight is plotted against time for different pH values, and there is no significant difference between the three plots. The kinetic constants are thought to follow the Arrhenius law

$$k_{di} = A_{di} \exp(-E_{di}/RT) \quad 1 \leq i \leq 3 \quad (22)$$

The kinetic constants  $k_{di}$  are estimated from experimental data by minimizing the quadratic difference between the experimental and the computed curves of degradation concentration against time [16]. We note that only  $k_{d1}$  is involved in Eq. (18),  $k_{d1}$  and  $k_{d2}$  in Eq. (19), and  $k_{d2}$  and  $k_{d3}$  in Eqs. (20) and (21). Then the three constants can be successively determined by minimizing the objective functions  $f_i$  ( $1 \leq i \leq 3$ )

$$f_i = - \sum_{k=1}^N [\rho_{i,\text{exp}}(k) - \rho_{i,\text{cal}}(k)]^2 \quad (23)$$

where  $N$  denotes the number of experimental points, and  $\rho_{i,\text{exp}}$  (or  $\rho_{i,\text{cal}}$ ) is the experimental (or calculated) mass concentration of species of class  $i$ .

The logarithms of the raw  $k_{di}$  values are then plotted against the inverse of temperature (Fig. 8) to determine the activation energies  $E_{di}$  and the pre-exponential factors  $A_{di}$  (in  $\text{s}^{-1}$ )

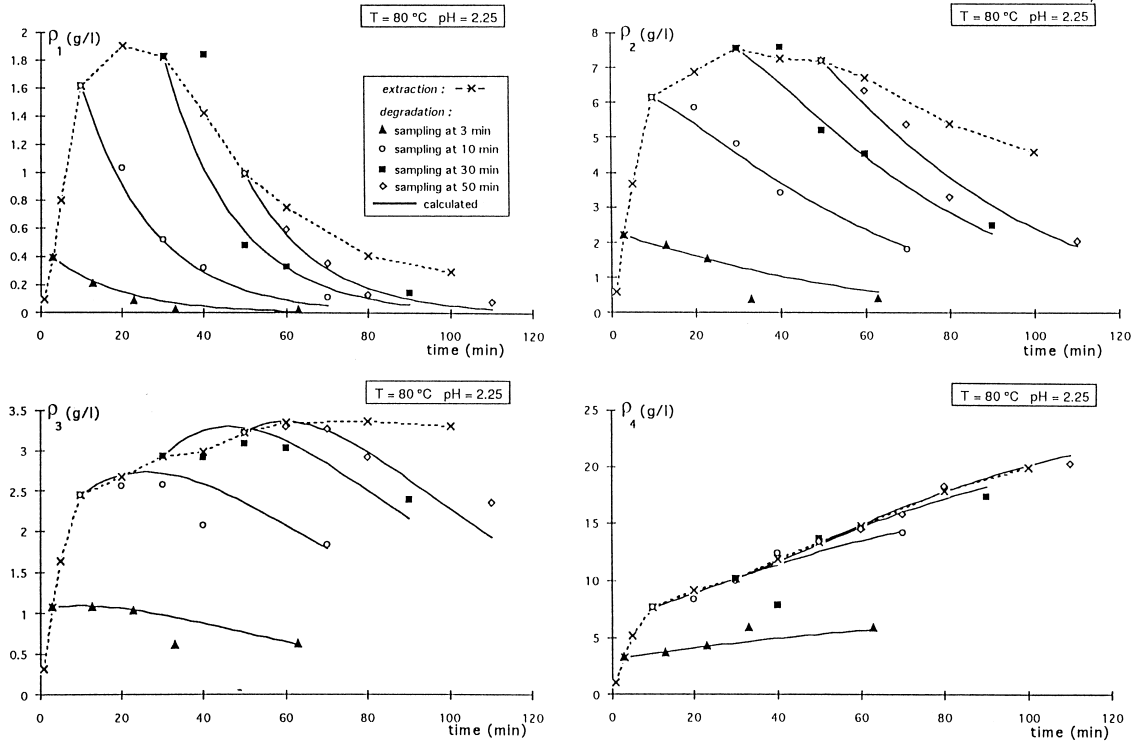


Fig. 9. Experimental and calculated mass concentration of the four classes of gelatin versus time during a degradation experiment performed at 80 °C and pH 2.25. The evolutions of samples taken at 3, 10, 30 and 50 min are plotted.

$$k_{d1} = 5.880 \times 10^{11} \exp\left(-\frac{99914}{RT}\right) \quad (24)$$

$$k_{d2} = 9.907 \times 10^7 \exp\left(-\frac{76819}{RT}\right) \quad (25)$$

$$k_{d3} = 7.552 \times 10^5 \exp\left(-\frac{61287}{RT}\right) \quad (26)$$

The  $E_{di}$  values agree with those quoted by Veis [17], and range from 75 to 92 kJ mol<sup>-1</sup>.

Knowing  $k_{di}$ , the evolution of the mass concentration of each class during degradation can be predicted. An example is given in Fig. 9, where the experimental and calculated  $\rho_{i(1 \leq i \leq 4)}$  are plotted versus time at 80 °C and pH 2.25; the initial concentrations correspond to samples taken during extraction at times of 3, 10, 30 and 50 min.

A good agreement between experimental and computed values is observed. The point is that, despite the complexity of the problem, a simple kinetic model involving only three degradation reactions gives a sufficient representation of reality.

#### 4.3. Determination of the kinetic constants of extraction reactions

For the overall operation (including extraction and degradation), the mass balances of the four classes include both extraction and degradation reactions (Eqs. (27)–(30)). The degradation kinetics are written as explained in Eqs. (18)–(21) and the extraction kinetics are written in a fashion sim-

ilar to Eq. (2), that is to say, the shrinking-core model with chemical reaction as the limiting step.

$$\frac{d\rho_1}{dt} = k_{e1} a_0 \rho_0 \left(1 - \frac{\sum \rho_i}{\rho_0}\right)^{\alpha_1} - k_{d1} \rho_1 \quad (27)$$

$$\frac{d\rho_2}{dt} = k_{e2} a_0 \rho_0 \left(1 - \frac{\sum \rho_i}{\rho_0}\right)^{\alpha_2} - k_{d2} \rho_2 + 3 \frac{\bar{M}_{w2}}{\bar{M}_{w1}} k_{d1} \rho_1 \quad (28)$$

$$\frac{d\rho_3}{dt} = k_{e3} a_0 \rho_0 \left(1 - \frac{\sum \rho_i}{\rho_0}\right)^{\alpha_3} - k_{d3} \rho_3 + 2 \frac{\bar{M}_{w3}}{\bar{M}_{w2}} k_{d2} \rho_2 \quad (29)$$

$$\frac{d\rho_4}{dt} = k_{e4} a_0 \rho_0 \left(1 - \frac{\sum \rho_i}{\rho_0}\right)^{\alpha_4} + \frac{\bar{M}_{w4}}{\bar{M}_{w2}} k_{d2} \rho_2 + 3 \frac{\bar{M}_{w4}}{\bar{M}_{w3}} k_{d3} \rho_3 \quad (30)$$

The extraction kinetics depend on both temperature and pH, and so we chose to write the constants in the form

$$k_{ei} a_0 = k_{appi} \exp\left(-\frac{E_{ei}}{RT}\right) \quad (31)$$

$$k_{appi} = A_{ei} [H^+]^{\alpha_i}$$

In this way, the initial area  $a_0$  of the ossein pellets is taken into account (it is easy to adapt the constant value if the pellet size is changed). This is merely a question of notation, and could be noted by  $k_{ei}$ . The pre exponential factor  $k_{appi}$  depends on  $[H^+]$ .

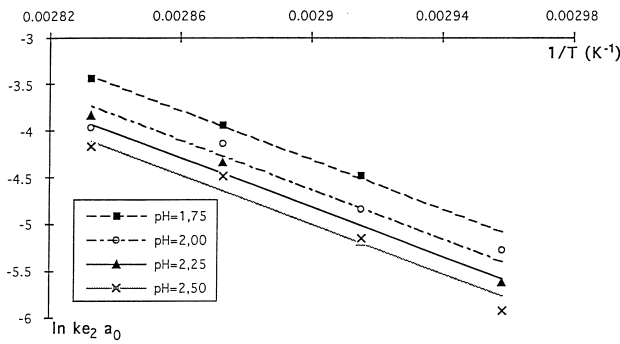


Fig. 10. Determination of the activation energy of the extraction reactions: plot of the logarithms of the rate constants (extraction of the second class) versus the inverse of temperature for pH 1.75, 2.00, 2.25 and 2.50.

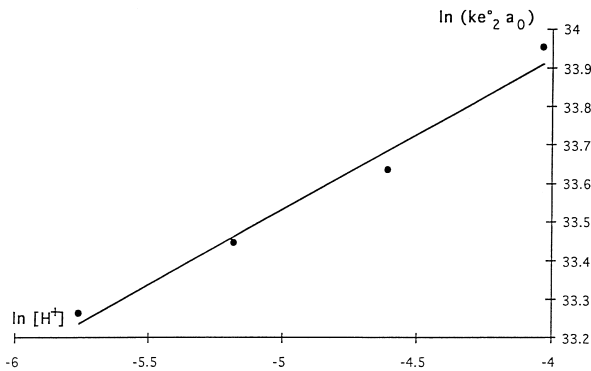


Fig. 11. Example of the determination of  $A_{ei}$  and  $\alpha_i$  of the pre-exponential factor of the constant rate of extraction reaction (extraction of the second class) versus  $\ln[H^+]$ .

Table 5  
Parameters  $A_{ei}$ ,  $\alpha_i$  and  $E_{ei}$  of the extraction kinetic laws

$i$	$A_{ei}/\text{kg s}^{-1} (\text{mol m}^{-3})^{-\alpha_i}$	$\alpha_i$	$E_{ei}/(\text{J mol}^{-1})$
1	$5.831 \times 10^{17}$	0.40	140423
2	$4.492 \times 10^{13}$	0.40	109678
3	$6.917 \times 10^7$	0.33	75208
4	$1.293 \times 10^{12}$	0.33	100682

The  $k_{ei}a_0$  values are obtained by an optimization procedure, as was done previously for degradation. Then, to determine  $A_{ei}$ ,  $\alpha_i$  and  $E_{ei}$ , the logarithms of  $k_{ei}a_0$  are plotted against inverse temperature for each pH; an example is presented in Fig. 10. This gives the values of  $E_{ei}$  and of  $A_i[H^+]^{\alpha_i}$ . To compute the  $A_{ei}$  and  $\alpha_i$  values, the logarithm of  $A_{ei}[H^+]^{\alpha_i}$  is plotted versus  $\ln[H^+]$  (Fig. 11). The results are given in Table 5. The exponents  $\alpha_i$  are almost the same for the four product classes (it would have been similar to suppose that the four extraction reactions had an order  $\alpha_i$  with respect to  $[H^+]$ , instead of including  $[H^+]$  in the constants).

The experimental and computed variations of  $\rho_i$  against time are plotted for different pH values at 80 °C, and one example is given in Fig. 12. Good agreement is observed between experimental and computed values.

These results show that the kinetic model that has been proposed allows a description of the evolution of the mass

concentrations of each category of product with fairly good precision.

#### 4.4. Discussion

The first part has shown that extraction proceeds in a shrinking-core fashion and that chemical reaction is the controlling step. A kinetic constant  $k$  has been determined for the experimental conditions (mean radius 0.20–0.75 mm, pH 2.25, 75 °C). In the second part, the rate-limiting step is the same; the products are divided into four classes and degradation reactions are taken into account. Expressions for the kinetic constants have been proposed as a function of temperature and pH. To check the consistency, let us compare the value of  $k$  with the value that would be obtained for an overall constant in the second part. Degradation reactions are not taken into account (because these reactions do not alter the overall gelatin concentration). What must be compared is Eq. (2)

$$\frac{dX_B}{dt} = \frac{3k}{\rho_B R_0} (1 - X_B)^{\frac{2}{3}}$$

$$X_B = \rho / \rho_0$$

with the sum of Eqs. (27)–(30) without the degradation terms, and

$$\frac{d\rho}{dt} = a_0 \rho_0 \sum_{i=1}^4 k_{ei} \left( 1 - \frac{\sum_{i=1}^4 \rho_i}{\rho_0} \right)^{\frac{2}{3}} \quad (32)$$

Then, by identification, we must have

$$\frac{3k}{\rho_B R_0} = a_0 \sum_{i=1}^4 k_{ei}$$

In the first part, the pH is 2.25 and the temperature is 75 °C; this would give

$$a_0 \sum_{i=1}^4 k_{ei} = 5.01 \times 10^{-4} \text{ s}^{-1} \quad (34)$$

and

$$\frac{3k}{\rho_B R_0} = 2.27 \times 10^{-4} \text{ s}^{-1} \quad (\text{since } R_0 = 0.37 \text{ mm}) \quad (35)$$

The ratio of the values from Eqs. (34) and (35) is 2.2: it is the same order of magnitude. It would not have been possible to obtain exactly the same value because the raw materials are not the same, and it is logical to find that

$$a_0 \sum_{i=1}^4 k_{ei} > \frac{3k}{(\rho_B R_0)}$$

because extraction is easier from ossein than from hard bones. There is good consistency between the two types of results.



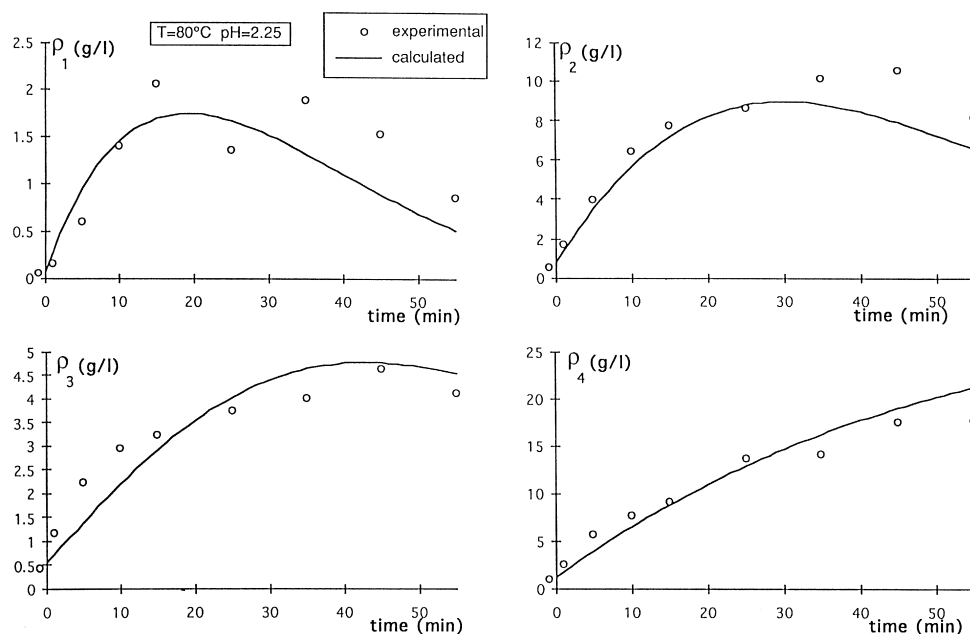


Fig. 12. Experimental and calculated evolution of the mass concentration of the four classes of gelatin versus time,  $T = 80^\circ\text{C}$ ,  $\text{pH} = 2.25$ . (The point  $t < 0$  corresponds to a measurement made before the reaction).

## 5. Conclusion

In this paper, two parts were presented.

The extraction of gelatin from hard bones was studied experimentally at  $75^\circ\text{C}$  and  $\text{pH} 2.25$  for different particle sizes. Results were interpreted in the frame of the shrinking-core model. It was shown that chemical reaction was the limiting step and a global kinetic constant  $k$  was computed.

The scope was then to build an overall kinetic scheme. It was assumed that the products could be divided into four classes and that there were four extraction reactions and three degradation reactions of the longest chains. The kinetic laws were then determined as functions of temperature and  $\text{pH}$  (in the range  $T = 65\text{--}80^\circ\text{C}$  and  $\text{pH} 1.75\text{--}2.50$ ).

The results obtained with this approach allowed us to model the variations of the mass concentrations of the four classes and thus the yield and mean molecular weight of the gelatin produced. This model would apply over a more extended  $\text{pH}$  and temperature range and with other raw materials, and some experiments should be performed to determine the appropriate constants. This is relatively simple but gives a correct prediction and can be easily integrated into a complete model of gelatin production.

What is especially interesting here is the methodology. At the beginning of the study, numerous experimental data were available. The problems were tackled with a chemical engineering approach: in the first part a well known model was used, and in the second part simplifying assumptions were made in order to construct a phenomenological kinetic scheme. Finally, answers have been proposed that are sufficient for the moment and could be used to design continuous reactors.

## 6. Nomenclature

$A_{i(1 \leq i \leq 4)}$	class of product number $i$
$A_{ei}$	pre-exponential factor of the extraction constant $k_{ei}a_0$ ( $\text{kg s}^{-1} (\text{mol m}^{-3})^{-\alpha_i}$ )
$A_{di}$	pre-exponential factor of the degradation constant $k_{di}$ ( $\text{s}^{-1}$ )
$a_0$	specific area of the particles ( $\text{m}^2 \text{g}^{-1}$ )
$C_A$	concentration of $\text{H}^+$ in the bulk ( $\text{mol m}^{-3}$ )
$C_{AS}$	concentration of $\text{H}^+$ at the particle surface ( $\text{mol m}^{-3}$ )
$d$	particle diameter (m)
$D_A$	molecular diffusivity of $\text{H}^+$ ( $\text{m}^2 \text{s}^{-1}$ )
$D_e$	effective diffusivity of $\text{H}^+$ in the particle ( $\text{m}^2 \text{s}^{-1}$ )
$E_{di}$	activation energy of the degradation reactions ( $\text{J mol}^{-1}$ )
$E_{ei}$	activation energy of the extraction reactions ( $\text{J mol}^{-1}$ )
$F_A$	molar flux of $\text{H}^+$ ( $\text{mol s}^{-1}$ )
$f_i$	objective functions for optimization ( $1 \leq i \leq 3$ )
$[\text{H}^+]$	concentration of $\text{H}^+$ ( $\text{mol m}^{-3}$ )
$k$	extraction rate constant ( $\text{kg s}^{-1} \text{m}^{-2}$ )
$k_{appi(1 \leq i \leq 4)}$	apparent rate constant of degradation reactions ( $\text{s}^{-1}$ )
$k_d$	external transfer conductance ( $\text{m s}^{-1}$ )
$k_{di(1 \leq i \leq 3)}$	rate constants of degradation reactions ( $\text{s}^{-1}$ )
$k_{ei(1 \leq i \leq 4)}$	rate constants of extraction reactions per unit of surface ( $\text{g s}^{-1} \text{m}^{-2}$ )
$M_B$	mean molecular weight of gelatin ( $\text{kg m}^{-3}$ )

$m_B$	mass of gelatin still present in a particle at $t$ (kg)
$m_{B0}$	initial mass of gelatin available in a particle (kg)
$M_{wi}$	mean molecular weight of class $i$ ( $\text{g mol}^{-1}$ )
$N$	number of experimental points
$R$	core radius (m)
$R_0$	particle radius (m)
Re	Reynolds number
Sc	Schmidt number
Sh	Sherwood number
$t$	current time (s)
$T$	temperature (K)
$X_B$	conversion
$\alpha_i$	exponent of $[\text{H}^+]$ in the equation giving $k_{ei}a_0$
$\gamma$	proportionality factor between $k_d$ and $R_0^{-1/2}$ ( $\text{m}^2 \text{s}^{-1}$ )
$\lambda_1$	model parameter when extraction is under chemical control ( $\text{s m}^{-1}$ )
$\lambda_2$	model parameter when extraction is under external transfer control ( $\text{s m}^{-3/2}$ )
$\lambda_3$	model parameter when extraction is under internal diffusion control ( $\text{s m}^{-2}$ )
$\nu_{ji}$	stoichiometric coefficient of class $i$ ( $1 \leq i \leq 4$ ) in the degradation reaction number $j$ ( $1 \leq j \leq 3$ )
$\rho_0$	mass concentration of gelatin initially in the particle ( $\text{g m}^{-3}$ )

$\rho_B$	apparent density of gelatin ( $\text{kg m}^{-3}$ )
$\rho_i$	mass concentration of class $i$ ( $\text{g m}^{-3}$ )

## References

- [1] H.G. Curme, T.H. James (Ed.), The Theory of the Photographic Process, 4th edn., Macmillan, New York, 1977, p. 45.
- [2] R.J.A. Grand, G. Stainsby, J. Sci. Food Agric. 26 (1975) 295.
- [3] M.Z. Huang, J.K. Miao, C. Zhang, Gelatin Proc. IAG Conf. 5th, 1988, p. 184.
- [4] J. Alleavitch, A.W. Turner, C. Finch, Gelatin, Ullmann's Encyclopedia of Industrial Chemistry, A12, 5th edn., 1989, p. 307.
- [5] Eastman Kodak Corp., Gelatin, US Patent 2 460 809.
- [6] W. Kowal, Fleisch-Ind. USSR 4 (1951) 18.
- [7] L. Oudem, Swiss Patent 595 430, 1978.
- [8] B.T. Petersen, J.R. Yates, Ger. Offen, Br. Patent 2 629 594, 1977.
- [9] P.-J. Xia, W.-F. Zhao, Y.-B. Mo, X.-M. Ren, JIST 37 (4) (1993) 355.
- [10] W.-F. Zhao, Y.-B. Mo, P.-J. Xia, X.-M. Ren, JIST 37 (4) (1993) 359.
- [11] P.J. Markarewicz, L. Harasta, S.L. Webb, J. Photogr. Sci. 28 (1980) 177.
- [12] S. Yagi, D. Kunii, in The Combustion Institute (ed.), 5th Int. Symp. on Combustion: Combustion in Engines and Combustion Kinetics, Pittsburgh, Pennsylvania, Aug. 30–Sept. 3, 1954, Reinhold, New York, 1955, p. 231.
- [13] O. Levenspiel, Chemical Reaction Engineering, 2nd edn., John Wiley & Sons, New York, 1972.
- [14] J. Skezely, J.E. Evans, H.Y. Sohn, Gas–solid reactions, Academic Press, London, 1976.
- [15] W.E. Ranz, W.R. Marshall, Chem. Eng. Prog. 48 (1952) 141.
- [16] M.J. Box, Comput. J. 8 (1965) 42.
- [17] A. Veis, The Macromolecular Chemistry of Gelatin, Academic Press, New York, 1964.